

1 Proceedings

2 Using Thermal Neutron Imaging in Forest Products 3 Research †

4 Nayomi Z. Plaza^{1*}, Rebecca E. Ibach¹, Laura Hasburgh², Michael Taylor³

5 ¹ Forest Biopolymers Science and Engineering, USDA Forest Service, Forest Products Laboratory, One
6 Gifford Pinchot Dr., Madison, WI 53726, USA; rebecca.e.ibach@usda.gov

7 ² Building and Fire Sciences, USDA Forest Service, Forest Products Laboratory, One Gifford Pinchot Dr.,
8 Madison, WI 53726, USA; laura.e.hasburgh@usda.gov

9 ³ Phoenix Neutron Imaging Center, 5125 Lacy Rd, Fitchburg, WI 53711, USA;
10 michael.taylor@phoenixwi.com

11 * Correspondence: nayomi.plazarodriguez@usda.gov

12 † Presented at the 1st International Electronic Conference on Forests, 15–30 November 2020;

13 Available online: <https://sciforum.net/conference/IECF2020>

14 Published:

15 **Abstract:** Neutron imaging is a non-destructive evaluation technique with enhanced hydrogen
16 sensitivity that allows researchers to monitor water content and transport in materials. In
17 lignocellulosic research, this technique has typically been used to measure changes in moisture
18 content, water transport and even local changes in the density of wood. Yet, studies looking into the
19 combined effects of moisture-uptake, chemical modifications and thermal degradation are still
20 lacking. This is perhaps due to the inherent limited availability of these instruments and their lesser
21 spatial resolution compared to x-ray imaging. While recent advances in detector technology and
22 neutron production have led to continued improvements in both instrument availability and spatial
23 resolution, the technique remains underutilized in forests products research. Here, we used thermal
24 neutron imaging to measure differences in the attenuation of the neutron beam due to acetylation
25 in both solid wood samples and wood-plastic composite samples, as well as a thermally degraded
26 wood sample. Our results show that moisture plays a key role in the contrast. Moreover, we showed
27 that the attenuation coefficient is particularly sensitive to changes in density and/or local hydrogen
28 content caused by thermal degradation of the wood polymers.

29 **Keywords:** neutron imaging; radiography; thermal degradation; acetylated wood

30

31 1. Introduction

32 There is an increased interest in the use of forest products for construction beyond low-rise,
33 residential purposes due to their sustainability and ability to sequester carbon [1]. Yet, when used
34 outdoors these products are subject to various environmental conditions that can compromise their
35 long-term durability. Non-destructive evaluation that can provide insights on how forest products'
36 material properties are affected by these conditions could be valuable in accelerating the
37 development of effective and environmentally friendly protection systems. However, characterizing
38 wood and other lignocellulosic materials is difficult because of their inherently complex chemistry
39 and hierarchical structure. Moreover, the contrast between the polymeric constituents is often poor.

40 Neutron-based technologies are uniquely suited to probe lignocellulosic materials because
41 neutrons interact with the sample nuclei and have no dependence with the atomic number [2].
42 Neutron imaging (also referred to as neutron radiography in the literature) can be used to non-
43 destructively study the bulk distribution of moisture and other hydrogen-rich components with sub-
44 mm spatial resolution depending on the source and detector technology used [3]. Thus, this technique

45 is becoming an important tool in cultural heritage research of ancient artifacts including pottery,
46 metal clad statues and even fossilized woods [3,4]. Its high sensitivity to hydrogen content makes
47 thermal neutron imaging (TNI) a powerful tool to evaluate how forest products are chemically
48 modified as well as how they degrade. Despite its potential, the technique has not been widely used
49 in wood and forest products research. The limited existing research has focused on investigating
50 moisture uptake and water transport effects in various wood-based products [5–8], including wood-
51 plastic composites [9]. While, others have used the technique to measure local density variations
52 across growth rings [10]. More recently, cold neutron imaging has been used to monitor the *in-situ*
53 changes caused by thermal modification [11] and pyrolysis of wood [12].

54 In this manuscript, we give an overview on the use of TNI in a variety of forest products
55 including unmodified and acetylated solid wood and wood-plastic composites, as well as thermally
56 degraded wood. These materials were selected because of their use as outdoor products that need to
57 withstand the elements. Acetylation was selected because it is a commercial non-toxic wood
58 modification that is used for improving the decay resistance of these products. We also studied a
59 sample exhibiting a thermal degradation profile to determine the potential of TNI in detecting
60 degradation-induced variances within a sample. Our results show that, by carefully controlling the
61 moisture content in these samples, the image contrast can be further improved to detect localized
62 defects. Furthermore, our data supports that TNI can be a powerful tool to assess degradation in
63 terms of decreased density or hydrogen content, since these directly impact the measured attenuation
64 coefficient. Thus, TNI may be particularly useful in assessing the efficacy of wood modification and
65 other protection treatments meant to prevent decay and degradation.

66 2. Materials and Methods

67 Acetylated wood sample: Southern pine (*Pinus spp.*) sapwood blocks (25.4 mm wide x 25.4 mm
68 long x 6.4 mm thick) were cut and dried at 105 °C in a forced draft oven for 24 hours and then
69 weighed. Acetylation was performed by immersing the blocks in acetic anhydride at 120 °C for 240
70 minutes in a glass reactor [13]. The acetylated sample was water-leached for 14 days to remove any
71 residues (acetic acid by-product) from the modification. The acetylation led to an average weight
72 percent gain of 19.8% as determined from its original oven-dried weight.

73 Thermally degraded wood sample: Thin sections (4 mm) of a Douglas fir (*Pseudotsuga menziesii*)
74 specimen were cut from a thermally degraded wood sample. The thermal degradation occurred by
75 exposing the radial surface of an oven-dried Douglas fir wood specimen (100 mm x 100 x 21 mm) to
76 a constant heat flux of 50 kW/m² using a cone calorimeter (FTT iCone Mini, East Grinstead, West
77 Sussex, UK) without piloted ignition. Once the temperature of the bottom surface reached 100°C, the
78 sample was removed from the cone calorimeter, and the fire on the top surface was extinguished
79 with water. Then, the specimen was cut along the transverse plane into 4 mm thick sections to expose
80 the changes caused by the thermal degradation across various growth rings.

81 Wood-plastic composites (WPCs): The WPCs were made from high-density polyethylene
82 (HDPE) from reprocessed milk bottles (Muehlstein and Co., Inc., Roswell, Georgia), and ponderosa
83 pine (*Pinus ponderosa*) flour (AWF-4020), nominal 40 mesh (420 µm), from American Wood Fiber
84 (Schofield, Wisconsin). Adding 6 or 7.8% TPW-113 lubricant from Struktol Company of America
85 (Stow, Ohio) helped prevent tearing of the material as it exited the die [14]. To produce the WPCs,
86 the HDPE was melted, and blended with the wood flour and the lubricant. Then, the material was
87 extruded thru a die into rectangular specimens (3 mm thick x 13 mm wide x 76 mm long). For the
88 acetylated WPCs, the wood flour was oven dried and then boiled in acetic anhydride in a 1-L glass
89 reactor for 4 h to increase its acetyl content. The treated flour was washed and oven dried, and its
90 weight gain percentage (WPG) was calculated. Percentage acetyl content was determined using anion
91 exchange high-performance liquid chromatography with a suppressed conductivity detector,
92 following a previously described methodology [15]. The average acetyl content of the acetylated flour
93 was 22.65% ± 0.01 (average of 24 batches) while the unmodified flour was 1.95% ± 0.00 (average of 4
94 samples.)

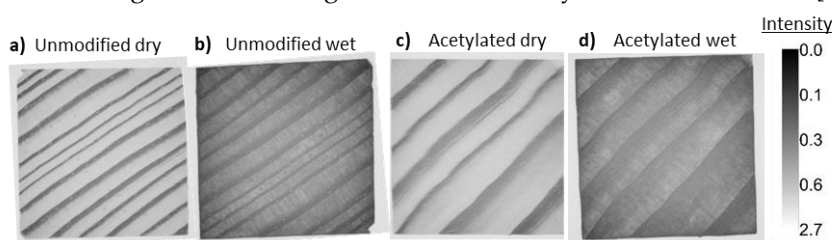
95 Neutron imaging: Experiments were conducted at one of the thermal neutron beamlines
 96 available at the Phoenix Neutron Imaging Center. Two-dimensional neutron radiography using
 97 conventional X-ray films in contact with high-resolution neutron conversion screens were used to
 98 measure the effects of moisture content and local density variations in the test specimens. First, all
 99 the samples were imaged dry at the beamline room conditions. The samples were fastened onto the
 100 plates using Al tape, exposed to thermal neutrons for 1.5 hours and were safe to handle immediately
 101 afterward. A week later, the same samples were soaked in water for over 24 hours, patted dry to
 102 remove the excess water and wrapped in aluminum foil to keep their moisture content stable. Then,
 103 the wrapped samples were imaged again using the thermal neutron beam. The increase in water
 104 content due to the immersion was determined by comparing the weight of the air-dried samples and
 105 the unsealed wet samples at the end of the experiment. The average thickness of the dry and wet
 106 samples was also measured. The films were developed in a dark room and digitized for quantitative
 107 analysis. The digitized images were first flattened along the Z-axis. Then, these corrected images were
 108 imported into ImageJ [16] where linear profiles were drawn over regions of interest to calculate the
 109 macroscopic attenuation coefficient, Σ , for each sample based on Beer-Lamberts' law (1)

$$\Sigma = \frac{\ln\left(\frac{I_0}{I}\right)}{d} \quad (1)$$

110 where I_0 is the incident beam intensity, I is the transmitted beam intensity and d is the sample
 111 thickness. For the wood samples, linear profiles were drawn across several growth rings, and the
 112 transmitted intensity values were averaged over at least five rings to calculate the attenuation
 113 coefficient, Σ , based on Equation 1. For the WPCs, linear profiles were drawn along the length of the
 114 samples, and attenuation coefficients were calculated based on the average transmitted beam
 115 measured. All image processing and analysis was performed using the ImageJ tools in FIJI [17].

116 3. Results and Discussion

117 The neutron radiographs obtained from the unmodified and acetylated wood samples in both
 118 dry and wet conditions are shown in Figure 1. The weight of both the unmodified and the acetylated
 119 samples increased considerably after being immersed over 24 hours in water (112%, and 87% with
 120 respect to their dry weights, respectively). The contrast between the less-dense earlywood bands and
 121 the dense latewood bands is very high for all dry samples (Figures 1a and 1b), however, increasing
 122 the moisture content of the samples significantly reduced this contrast. Interestingly, unlike other
 123 imaging techniques such as X-ray computed tomography (XCT) or clinical magnetic resonance
 124 imaging (MRI), here the rings are still distinguishable in both dry and wet conditions [18].



125
 126 **Figure 1.** Digitized neutron radiographs obtained from unmodified wood at (a) dry and (b) wet
 127 conditions, and acetylated wood at (c) dry and (d) wet conditions.

128 Quantitative analysis revealed that the increase of moisture content in these samples increased
 129 their attenuation coefficient (Table 1). This was most noticeable in the less-dense earlywood regions
 130 probably because increasing the moisture content there led to a larger increase in the local apparent
 131 density. While the natural variability of wood likely contributes to the spread observed in the
 132 calculated attenuation coefficients, it should be noted that implementing normalization routines to
 133 account for deviations to the Beer-Lambert's law, such as a black body bias correction, can improve
 134 considerably the reproducibility and accuracy of the measured attenuation coefficient in

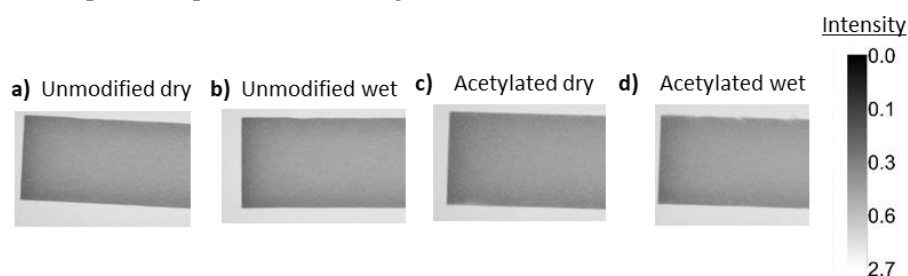
135 hydrogenous samples [19]. Thus, future experiments on wood samples may benefit from the use of
 136 post-processing normalization algorithms.

137 **Table 1.** Average macroscopic attenuation coefficients of the unmodified and acetylated wood at dry and
 138 wet conditions. Standard deviations are shown in parenthesis.

Sample	Σ (1/cm)	
	Dry	Wet
Unmodified Wood	0.86 (0.15) ¹	0.92 (0.33) ¹
	0.15 (0.04) ²	0.63 (0.21) ²
Acetylated Wood (20% WPG)	0.71 (0.16) ¹	0.75 (0.21) ¹
	0.16 (0.07) ²	0.60 (0.21) ²

139 ¹ Latewood. ² Earlywood

140 The radiographs obtained by imaging unmodified and acetylated WPCs in dry and wet
 141 conditioned are shown in Figure 2. Interestingly, for the WPCs we did not observe significant
 142 differences between the acetylated and the unmodified samples. Soaking these samples in water only
 143 increased their water content slightly (5% for the unmodified sample and 1% for the acetylated one
 144 compared to their dry weights). Therefore, it is not surprising that this small change did not yield
 145 observable differences. Future experiments with increased soaking times could increase the moisture
 146 content in these samples and provide new insights.



147
 148 **Figure 2.** Digitized neutron radiographs of WPCs made with unmodified wood flour imaged (a) dry
 149 and (b) wet, and WPCs made with acetylated wood flour imaged (c) dry and (d) wet.

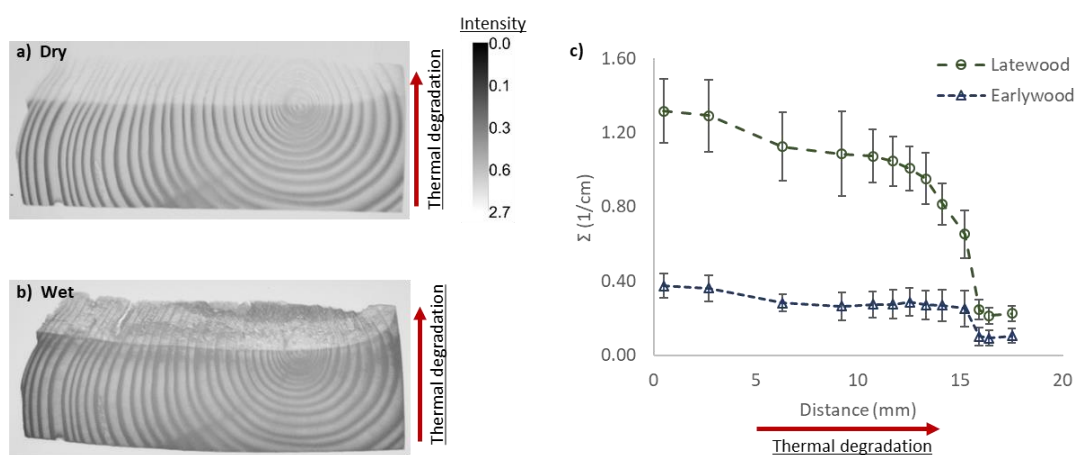
150 Quantitative image analysis along the length of the WPCs revealed that even though no
 151 significant differences were detected between the dry and wet samples, all samples were significantly
 152 more attenuated near the surfaces (Table 2). Possible explanations for this behavior include: the
 153 presence of a gradient in the materials properties due to the extrusion process used to fabricate the
 154 samples and/or that the wood fibers on the surface are more accessible to moisture [20] and thus more
 155 attenuated than the interior of the sample. However, considering the magnitude of the differences
 156 observed in our neutron images, further experiments and post-processing analysis that include black
 157 body bias corrections are likely needed to further confirm the presence of an attenuation gradient
 158 near the surfaces.

159 **Table 2.** Average macroscopic attenuation coefficients of the unmodified and acetylated WPCs at
 160 dry and wet conditions. Standard deviations are shown in parenthesis.

Sample	Σ (1/cm)	
	Dry	Wet
Unmodified WPC	1.18 (0.04) ¹	1.06 (0.20) ¹
	0.84 (0.07) ²	0.77 (0.06) ²
Acetylated WPC	1.31 (0.24) ¹	1.12 (0.20) ¹
	0.85 (0.07) ²	0.79 (0.05) ²

161 ¹ Surface regions. ² Non-surface areas

162 Soaking the thermally degraded sample in water over 24 hours increased its weight though not
 163 as much as the unmodified sample (60% vs. 112%, respectively). For the thermally degraded wood
 164 sample we observed that increasing the moisture content of the sample improved the contrast
 165 considerably and revealed the presence of cracks and defects that were otherwise indistinguishable
 166 (Figures 3a and 3b). The changes in the attenuation coefficient along the thermal degradation profile
 167 in the imaged dry sample are plotted in Figure 3(c). Interestingly, despite the low contrast in the dry
 168 sample, we still were able to observe a significant decrease in the attenuation coefficient with
 169 increased thermal degradation. Given that for wood, it is estimated that hydrogen accounts for nearly
 170 90% of the total attenuation [10,12], regardless of the neutron incident energy, it is likely that most of
 171 the decrease observed corresponds to a loss in the overall hydrogen content of the thermally
 172 degraded wood polymers. Considering that the attenuation is inherently dependent on the material's
 173 density it is conceivable that decreases in the wood's density as it is thermally degraded also
 174 contribute to attenuation loss.



175
 176 **Figure 3.** Digitized neutron radiographs obtained from a thermally degraded sample imaged (a) dry
 177 and (b) wet. (c) Plot showing the effects of thermal degradation on the average attenuation coefficients
 178 calculated from the dry sample shown in (a).

179 **4. Conclusions**

180 Thermal neutrons produced by a compact source were used to image various forest products.
 181 Using this tool, we investigated the combined effects of acetylation and moisture uptake on wood
 182 blocks and WPCs. We also investigated the effects of thermal degradation on a wood sample.
 183 Increasing the moisture content of the samples led to reduced contrast between the earlywood and
 184 latewood bands in both unmodified and acetylated wood samples. However, for the thermally
 185 degraded sample increasing the moisture content led to improved contrast that revealed new features
 186 and defects in the degraded regions. Our results show the enhanced hydrogen sensitivity of the
 187 technique makes it ideal to study the effects of degradation in wood and other forest products,
 188 particularly, in terms of local variations in the material's density or its hydrogen content.

190 **Author Contributions:** N.Z.P. conceived the paper, designed the experiments and analyzed the radiographs.
 191 M.T. collected the radiographs at the imaging center and digitized them. L.H. and R.I. prepared the samples.
 192 N.Z.P. wrote the paper with contributions from all authors.

193 **Funding:** This research received no external funding.

194 **Acknowledgments:** This research used one of the thermal neutron radiography beamlines at the Phoenix
 195 Neutron Imaging Center (PNIC) in Fitchburg, WI.

196 **Conflicts of Interest:** The authors declare no conflict of interest.

197 **References**

- 198 1. Jakes, J.E.; Arzola, X.; Bergman, R.; Ciesielski, P.; Hunt, C.G.; Rahbar, N.; Tshabalala, M.; Wiedenhoef, A.C.; Zelinka, S.L. Not Just Lumber—Using Wood in the Sustainable Future of Materials, Chemicals, and Fuels. *Jom* **2016**, *68*, 2395–2404. <https://doi.org/10.1007/s11837-016-2026-7>
- 199
- 200
- 201 2. Langan, P.; Evans, B.R.; Foston, M.; Heller, W.T.; O'Neill, H.; Petridis, L.; Pingali, S.V.; Ragauskas, A.J.; Smith, J.C.; Urban, V.S.; et al. Neutron Technologies for Bioenergy Research. *Ind. Biotechnol.* **2012**, *8*, 209–216. <https://doi.org/10.1089/ind.2012.0012>
- 202
- 203
- 204 3. *Neutron Methods for Archaeology and Cultural Heritage*; Kardjilov, N., Festa, G., Eds.; Neutron Scattering Applications and Techniques; Springer International Publishing: Cham, 2017; ISBN 978-3-319-33161-4; <https://doi.org/10.1007/978-3-319-33163-8>
- 205
- 206
- 207 4. Odin, G.P.; Rouchon, V.; Ott, F.; Malikova, N.; Levitz, P.; Michot, L.J. Neutron imaging investigation of fossil woods: Non-destructive characterization of microstructure and detection of in situ changes as occurring in museum cabinets. *Foss. Rec.* **2017**, *20*, 95–103. <https://doi.org/10.5194/fr-20-95-2017>
- 208
- 209
- 210 5. Sonderegger, W.; Hering, S.; Mannes, D.; Vontobel, P.; Lehmann, E.; Niemz, P. Quantitative determination of bound water diffusion in multilayer boards by means of neutron imaging. *Eur. J. Wood Wood Prod.* **2010**, *68*, 341–350. <https://doi.org/10.1007/s00107-010-0463-5>
- 211
- 212
- 213 6. Sonderegger, W.; Glaunsinger, M.; Mannes, D.; Volkmer, T.; Niemz, P. Investigations into the influence of two different wood coatings on water diffusion determined by means of neutron imaging. *Eur. J. Wood Wood Prod.* **2015**, *73*, 793–799. <https://doi.org/10.1007/s00107-015-0951-8>
- 214
- 215
- 216 7. Lanvermann, C.; Sanabria, S.J.; Mannes, D.; Niemz, P. Combination of neutron imaging (NI) and digital image correlation (DIC) to determine intra-ring moisture variation in Norway spruce. *Holzforschung* **2014**, *68*, 113–122. <https://doi.org/10.1515/hf-2012-0171>
- 217
- 218
- 219 8. Sedighi Gilani, M.; Abbasion, S.; Lehmann, E.; Carmeliet, J.; Derome, D. Neutron imaging of moisture displacement due to steep temperature gradients in hardwood. *Int. J. Therm. Sci.* **2014**, *81*, 1–12. <https://doi.org/10.1016/j.ijthermalsci.2014.02.006>
- 220
- 221
- 222 9. Islam, M.N.; Khan, M.A.; Alam, M.K.; Zaman, M.A.; Matsubayashi, M. Study of water absorption behavior in wood plastic composites by using neutron radiography techniques. *Polym. - Plast. Technol. Eng.* **2003**, *42*, 925–934. <https://doi.org/10.1081/PPT-120025004>
- 223
- 224
- 225 10. Mannes, D.; Lehmann, E.; Cherubini, P.; Niemz, P. Neutron imaging versus standard X-ray densitometry as method to measure tree-ring wood density. *Trees - Struct. Funct.* **2007**, *21*, 605–612. <https://doi.org/10.1007/s00468-007-0149-8>
- 226
- 227
- 228 11. Sonderegger, W.; Mannes, D.; Kaestner, A.; Hovind, J.; Lehmann, E. On-line monitoring of hygroscopicity and dimensional changes of wood during thermal modification by means of neutron imaging methods. *Holzforschung* **2015**, *69*, 87–95. <https://doi.org/10.1515/hf-2014-0008>
- 229
- 230
- 231 12. Ossler, F.; Santodonato, L.J.; Warren, J.M.; Finney, C.E.A.; Bilheux, J.C.; Mills, R.A.; Skorpenske, H.D.; Bilheux, H.Z. In situ monitoring of hydrogen loss during pyrolysis of wood by neutron imaging. *Proc. Combust. Inst.* **2019**, *37*, 1273–1280. <https://doi.org/10.1016/j.proci.2018.07.051>
- 232
- 233
- 234 13. Goldstein, I. S.; Jeroski, E. B.; Lund, A. E.; Nielson, J. F.; Weater, J.M. Acetylation of Wood in Lumber Thickness. *For. Prod. J.* **1961**, *11*, 363–370.
- 235
- 236 14. Ibach, R.E.; Clemons, C.M.; Schumann, R.L. WPCs with Reduced Moisture: Effects of Chemical Modification on Durability in the Laboratory and Field. In Proceedings of the 9th International Conference on Woodfiber-Plastic Composites, Madison Wisconsin, May 21-23, 2007, pp. 259–266.
- 237
- 238
- 239 15. Ibach, R.E.; Rowell, R.M.; Lee, B.-G. Decay Protection Based on Moisture Exclusion Resulting From Chemical Modification of Wood. In Proceedings of the 5th Pacific Rim Bio-Based Composites
- 240

- 241 Symposium, Canberra, Australia, December 10th-13th, 2000.; pp. 197–204.
- 242 16. Rasband, W.S., ImageJ, U. S. National Institutes of Health, Bethesda, Maryland, USA,
243 <https://imagej.nih.gov/ij/>, 1997-2018.
- 244 17. Schindelin, J.; Arganda-Carreras, I.; Frise, E.; Kaynig, V.; Longair, M.; Pietzsch, T.; Preibisch, S.; Rueden,
245 C.; Saalfeld, S.; Schmid, B.; et al. Fiji: An open-source platform for biological-image analysis. *Nat. Methods*
246 **2012**, *9*, 676–682. <https://doi.org/10.1038/nmeth.2019>
- 247 18. Mori, M.; Kuhara, S.; Kobayashi, K.; Suzuki, S.; Yamada, M.; Senoo, A. Non-destructive tree-ring
248 measurements using a clinical 3T-MRI for archaeology. *Dendrochronologia* 2019, *57*, 125630.
249 <https://doi.org/10.1016/j.dendro.2019.125630>
- 250 19. Carminati, C.; Boillat, P.; Schmid, F.; Vontobel, P.; Hovind, J.; Morgano, M.; Raventos, M.; Siegwart, M.;
251 Mannes, D.; Gruenzweig, C.; et al. Implementation and assessment of the black body bias correction in
252 quantitative neutron imaging. *PLoS One* 2019, *14*, 1–24. <https://doi.org/10.1371/journal.pone.0210300>
- 253 20. Gnatowski, M.; Ibach, R.; Leung, M.; Sun, G. Magnetic resonance imaging used for the evaluation of
254 water presence in wood plastic composite boards exposed to exterior conditions. *Wood Mater. Sci. Eng.*
255 *2015*, *10*, 94–111. <https://doi.org/10.1080/17480272.2014.920418>
- 256



© 2020 by the authors; licensee MDPI, Basel, Switzerland. This article is an open access article distributed under the terms and conditions of the Creative Commons Attribution (CC-BY) license (<http://creativecommons.org/licenses/by/4.0/>).